Supplementary Materials for

High photopiezocatalytic energy conversion via effective charge separation and deformability in the asymmetric ternary heterojunction $Bi_4Ti_3O_{12}$/PPy/TiO_2

Jialin Zhuang[a], Lingchao Wang[a], Yingmo Hu[a]*, Yechen Wang[a], Liping Lin[a], Jiaying Xiao[a], Yunfan Chen[a], Xiaowei Li[a], Huiqiang Liu[c], Qian Zhang[b]*, Qi An[a]*

a Engineering Research Center of Ministry of Education for Geological Carbon Storage and Low Carbon Utilization of Resources, Beijing Key Laboratory of Materials Utilization of Nonmetallic Minerals and Solid Wastes, National Laboratory of Mineral Materials, School of Materials Science and Technology, China University of Geosciences (Beijing), 100083, China

b School of Resources and Environment Engineering, Shandong University of Technology, Zibo, China.

c School of Physics and Optoelectronic Engineering, Shandong University of Technology, Zibo, China.

* Corresponding author. E-mail: (Y.H.) huyingmo@cugb.edu.cn, (Q.Z.) zq@sdut.edu.cn and (Q.A.) an@cugb.edu.cn.

Supplementary Text

1. Experimental section

1.1 Synthesis and characterization of BTO, TiO_2, MoS_2 and $BaTiO_3$

0.4 g of TiO_2 was added into 100 ml $(CH_3CH_2CH_2CH_2)_4N(OH)\cdot 10H_2O$ to obtain a mixture with the concentration of 0.253 mol/L. The mixture was stirred for 15 days to become a milky white suspension.

$Bi_3Ti_4O_{12}$ nanosheets (BTO) were prepared according to the reported hydrothermal method[1]. Specifically, 2.1 mmol of $Ti(OC_4H_9)_4$, 0.15 mol of NaOH, 2.8 mmol of $Bi(NO_3)_3\cdot 5H_2O$, and 0.1 mmol of $C_{18}H_{33}NaO_2$ were added into 30 ml ultrapure water and stirred 60 min. Afterwards, the mixture was transferred into a 50 mL sealed Teflon-lined autoclave and the solvothermal reaction was carried out at 180 °C for 15 h. The collected products were washed by ethyl ethanol and ultrapure water, and dried at 60 °C overnight. 0.2 g of BTO was added into 100 ml mixed solution of ethyl ethanol and water (by volume 1:1) and with ultrasonic treatment for 10 h.

0.2 g of MoS_2 and 0.2 g of $BaTiO_3$ were added to 100 ml of a mixture of ethanol and water (1:1, v/v), respectively, and sonicated for 10 h to obtain suspension.

1.2 Piezo-photocatalytic dye degradation and H_2O_2 generation experiment

0.05 g samples (copper mesh (49 mg) and catalyst (1 mg), obtained by subtracting the mass of copper mesh after assembly from the mass of copper mesh before assembly) were dispersed in 20 ml Rhodamine solution (RhB, 20 mg/L), methyl orange (MO, 10 mg/L), methylene blue (MB, 20 mg/L) and tetracycline hydrochloride (TC, 20 mg/L). After 30 min of dark adsorption, with different stirring speed (400 rpm) or ultrasonic vibration of 240 W power, the samples was exposed to 300 W Xenon lamp illumination (light intensity is 1 kW/m^2) to degrade RhB. Perform piezo-photocatalytic degradation for 2 h, and measure the absorbance of RhB every 30 min. In addition, when regulating the light intensity, the light intensity is set to 800, 1000 and 2000 W/m^2, respectively, and when regulating the ultrasound intensity, the ultrasound intensity is set to 120, 180, 240 and 300 W, respectively. In the experiment of regulating solution pH, solution pH was regulated by NaOH (1 M) and HCl (1 M) to obtain solutions with pH 3, 5, 7, 9 and 11, respectively.

0.05 g samples were dispersed in 20 ml ultrapure water. Under ultrasonic vibration and light illumination to generate H_2O_2. Use iodometry to determine the yield of H_2O_2 in the reaction process. 4 mL of the reaction suspension was taken out at an interval of

30 min and 500 μL of it after centrifugation treatment was diluted 5 times and mixed with 50 μL $H_{32}Mo_7N_6O_{28}$ solution with concentration of 0.01 M as well as 2 mL KI solution with concentration of 0.1 M. After reaction for 10 min, the absorbance intensity of the above mixture solution was recorded at 352 nm on an UV-Vis spectrophotometer to obtain the H_2O_2 concentration.

1.3 Calculation of d_{33} intensity

The d_{33} intensity ratios of BTO/PPy/TiO_2 and BTO/TiO_2 were obtained by calculating the butterfly curve of PFM. The calculation formula is:

$$d_{33} = m \times \frac{a}{VAC}$$

m: the inverse of the slope of the curve of the vertical coordinate of the force curve multiplied by the sensitivity of the probe;

a: measured amplitude of oscillation;

VAC: voltage applied to the sample.

2 Results and discussion

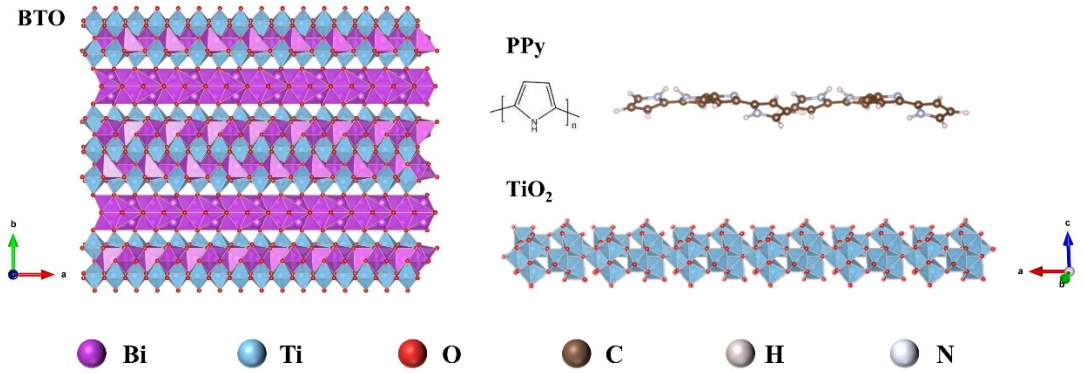

Fig. S1. Lattice schematic of BTO and TiO_2, structural formula and schematic of PPy. Applying stresses from a, b, and c axis directions respectively all lead to polarization of BTO[2].

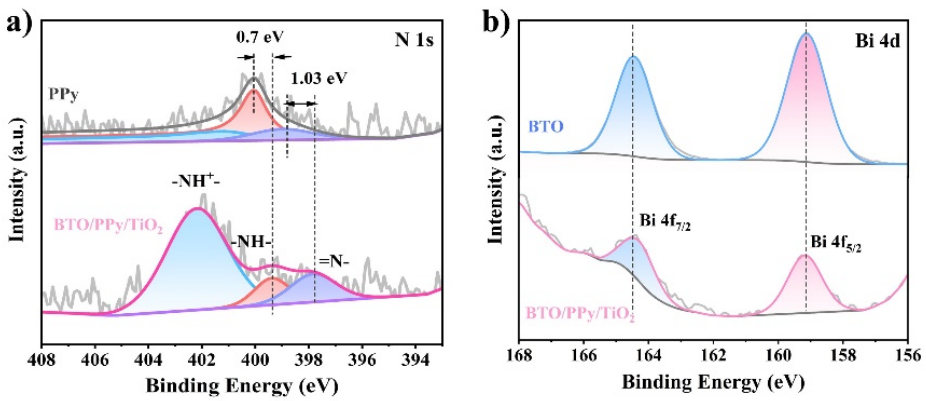

Fig. S2. XPS N 1s of PPy and BTO/PPy/TiO_2, XPS Bi 4d of BTO BTO/PPy/TiO_2.

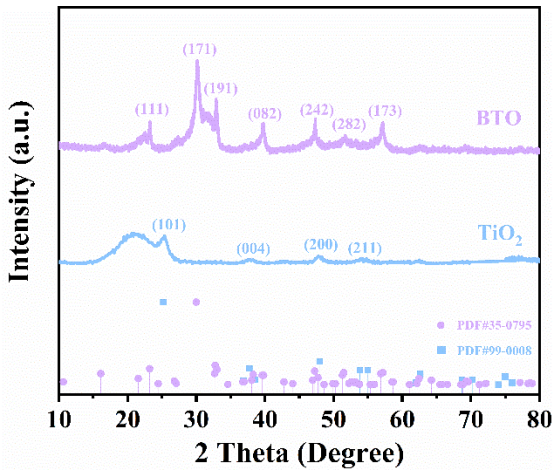

Fig. S3. XRD of TiO_2 and BTO.

XRD (Cu Kα radiation，λ = 0.15418 nm, Bruker D8) was applied to observe the phase structures of commercially purchased TiO_2 and BTO prepared by hydrothermal method. All the diffraction peaks of TiO_2 and BTO could be indexed to the hexagonal wurtzite phase of anatase TiO_2 (JCPDS Card No. 99-0008) and $Bi_4Ti_3O_{12}$ (JCPDS Card No. 35-0795), respectively.

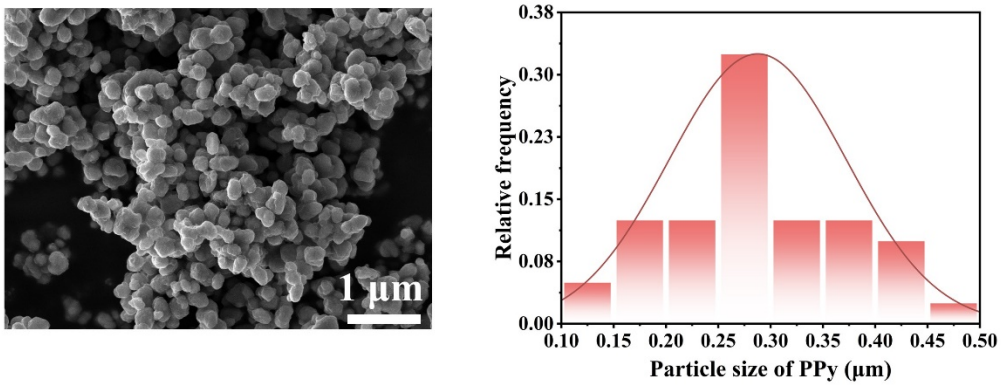

Fig. S4. SEM and particle size of PPy

As shown in SEM PPy is in granular form. The particle size was counted based on the SEM image and most of the PPy had a particle size of 250-300 nm.

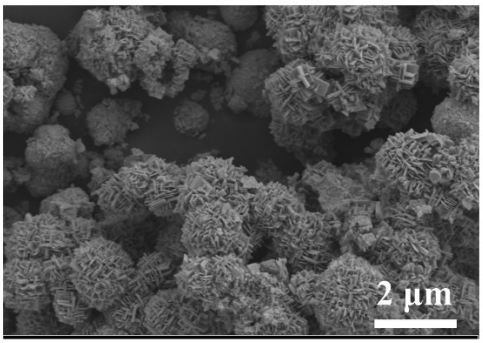

Fig. S5. SEM of BTO. BTO was in the form of nanocluster flower.

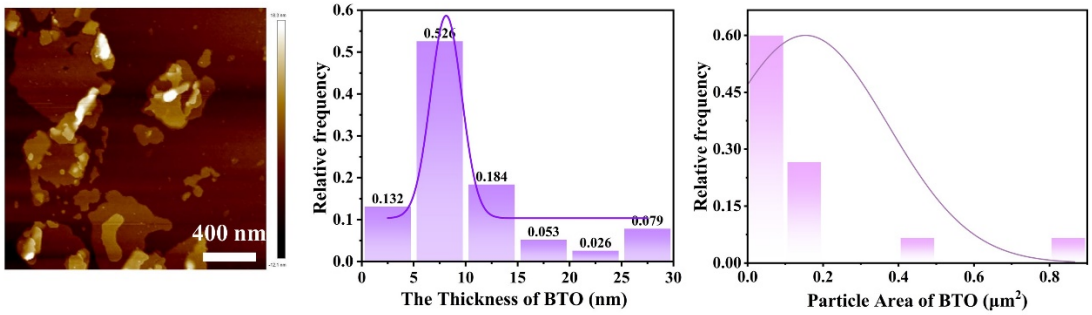

Fig. S6. AFM, thickness, and particle size of BTO.

The morphology and thickness of BTO after mechanical stripping were observed by AFM. The results show that the BTO was exfoliated into 2D nanosheets. The thickness and particle area distribution of the nanosheets were further counted, most BTO nanosheets had a thickness of 5-10 nm, and had a particle size of 0.1 μm^2.

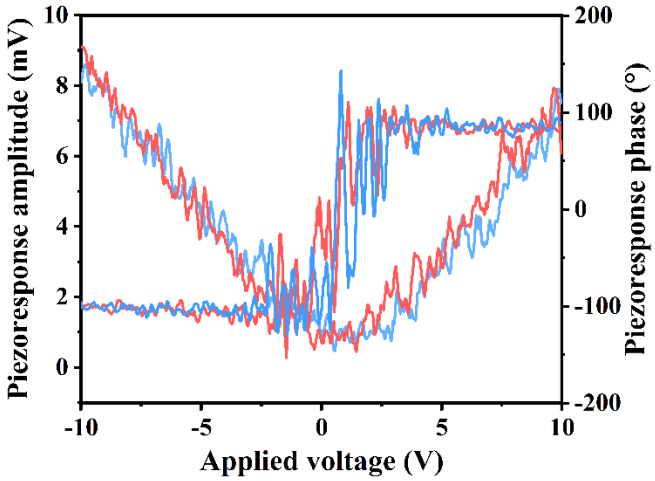

Fig. S7. butterfly amplitude loop and phase curve of BTO.

PFM tests were performed on the exfoliated BTO to detect its piezoelectric responsivity, and the BTO did not exhibit significantly separated phase curve and butterfly amplitude loop.

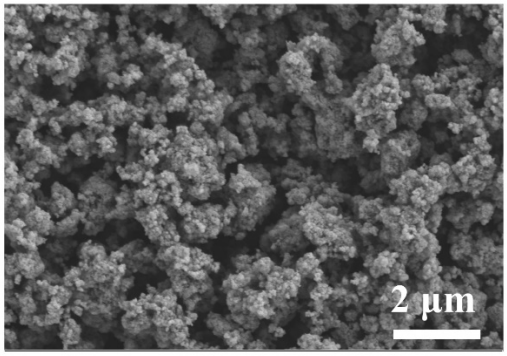

Fig. S8. SEM of TiO_2.

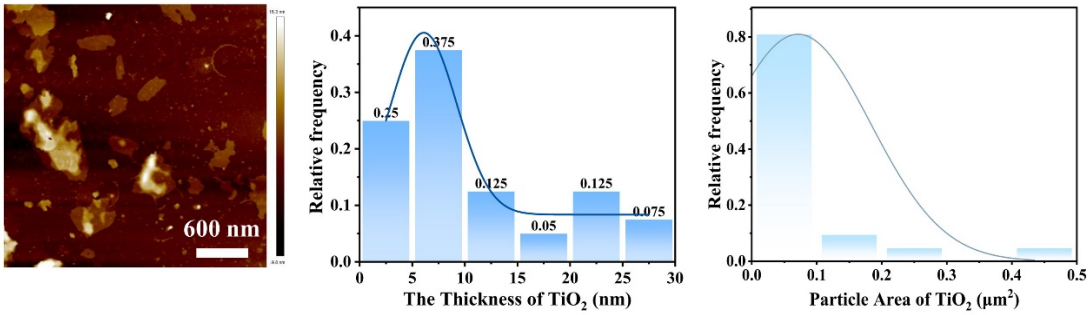

Fig. S9. AFM, thickness, and particle size of TiO_2.

The exfoliated TiO_2 was in the form of less-layered two-dimensional nanosheets as measured by AFM. The thickness and particle area distribution of the nanosheets were further counted, most TiO_2 nanosheets had a thickness of 5-10 nm, and had a particle size of 0.1 μm^2.

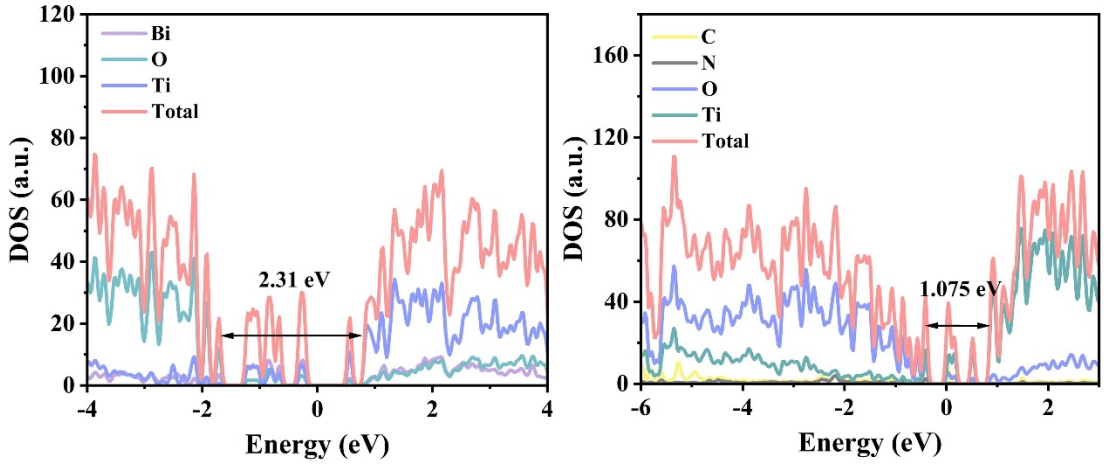

Fig. S10. DOS of BTO and PPy/BTO.

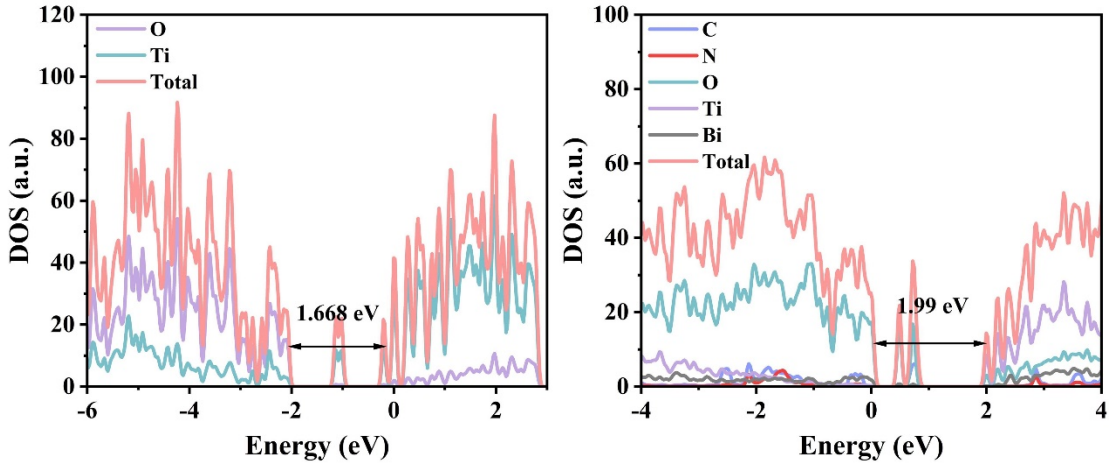

Fig. S11. DOS of TiO_2 and PPy/TiO_2.

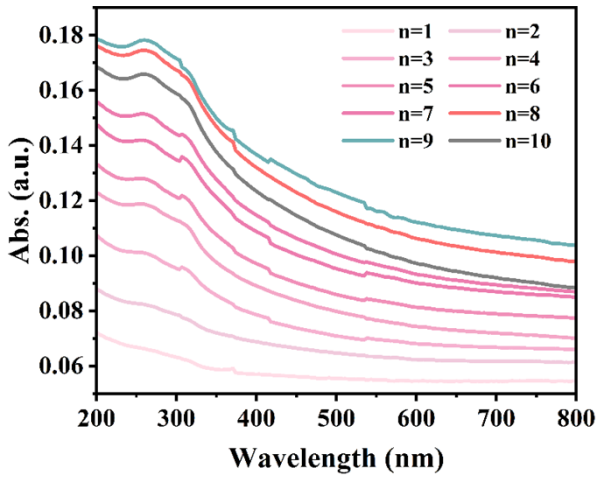

Fig. S12. UV-Vis absorption spectra of BTO/PPy/TiO_2 (n = 1~10).

The assembly process was monitored by UV-Vis spectrophotometer, and the gradual increase in absorbance with the increase in the number of assembled layers indicated that the components were successfully assembled onto the substrate surface. With the increase in the number of assembled layers (n), the absorbance reached its maximum value at n = 9 and was similar to the absorbance value at n = 8. With further assembly, when n = 10, catalyst detachment leads to a decrease in absorbance. In addition, previous studies have shown that the increase in the photogenerated carrier transfer paths with too many assembled layers results in unfavorable electron transfer to the catalyst surface and is not conducive to the utilization of the catalyst for light absorption. Therefore, the assembly of 8-layer was chosen for the experiment.

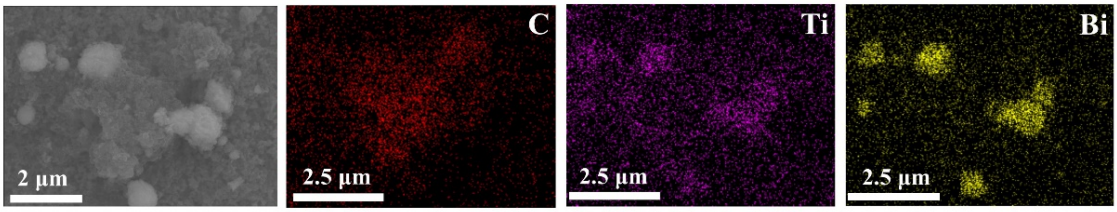

Fig. S13. SEM and elemental mapping images of BTO/PPy/TiO_2.

The results showed that PPy, TiO_2 and BTO were assembled to the surface of the copper mesh.

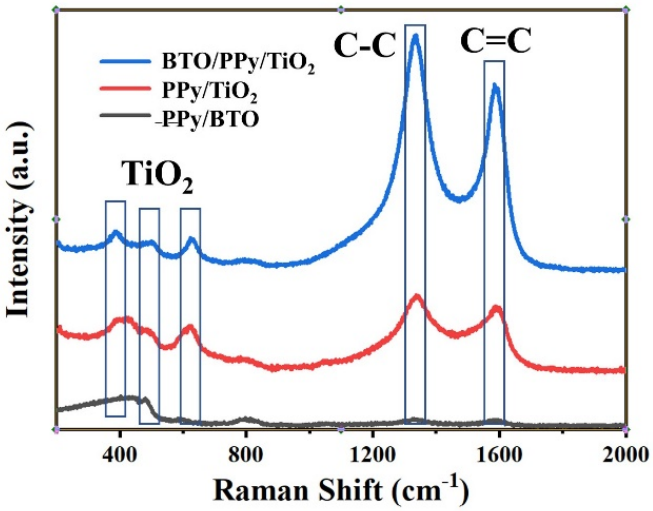

Fig. S14. Raman mapping of BTO/PPy/TiO_2、PPy/TiO_2 and PPy/BTO.

415、520 and 650 cm^{-1} corresponds to the Ti-O Raman vibrational peak. 1334 and 1590 cm^{-1} correspond to the C-C and C=C Raman vibrational peaks of PPy.

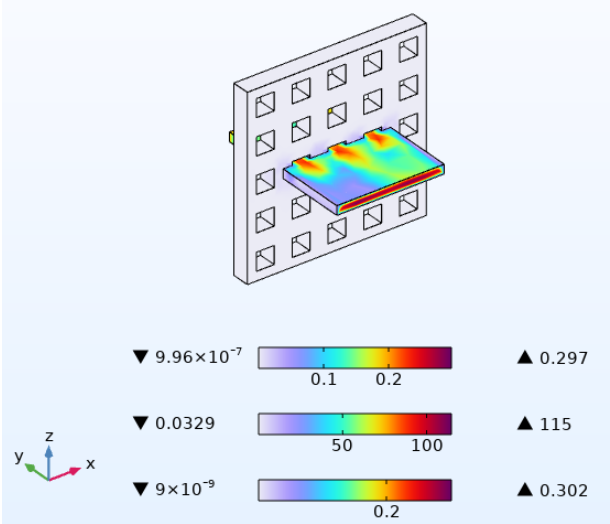

Fig. S15. COMSOL simulation of surface forces on mesh substrates under agitation. (Legend from top to bottom: tangential velocity magnitude (m/s), pressure (Pa), body velocity magnitude (m/s).)

According to the relationship between linear velocity and rotational speed, a brief estimation of the velocity of the solution hitting the catalyst and the copper mesh is obtained according to the equation:

$$v=\omega*2\pi r$$

When the rotational speed is 800 r/min, v=2 m/s. COMSOL simulations yielded a force of about 40 Pa on the surface of the copper mesh.

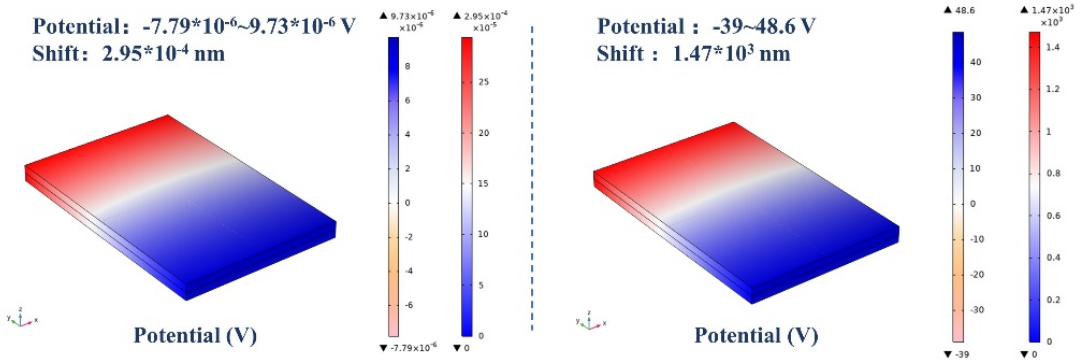

Fig. S16. COMSOL simulations were performed to calculate the surface forces on BTO/TiO_2 under stirring and the deformation of BTO/TiO_2 under different mechanical forces.

FES was set up in COMSOL Multiphysics®. In this model, the piezoelectric interface consists of a "Structural Mechanics Module" and an "Electrostatics Interface" coupled together by the multiphysical properties of the piezoelectric effect. The BTO (200×300×10 nm), and TiO_2 (200×300×10 nm) model is constructed based on AFM and SEM characterization. The stress on the surface of BTO/TiO_2 were obtained from FES calculations and references. FET simulation verifies that stirring causes much weak substrate deformation than ultrasonic treatment.

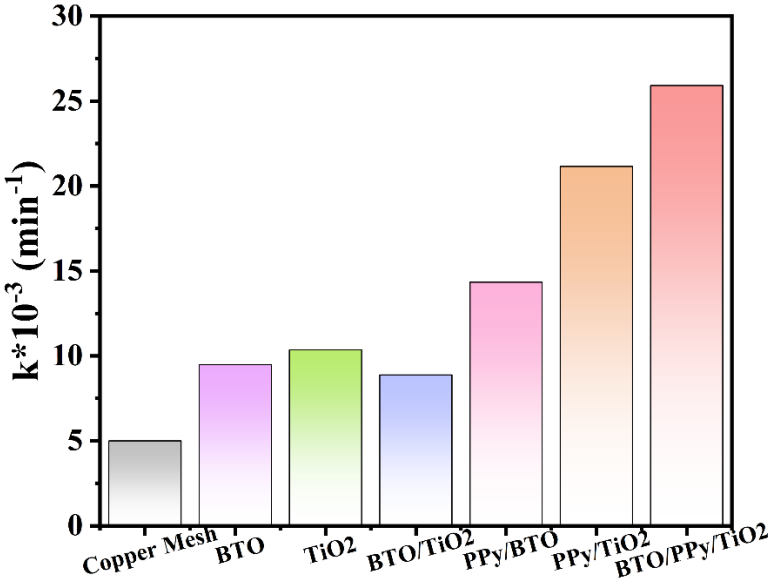

Fig. S17. First-order rate constant (k_{obs}) of different samples.

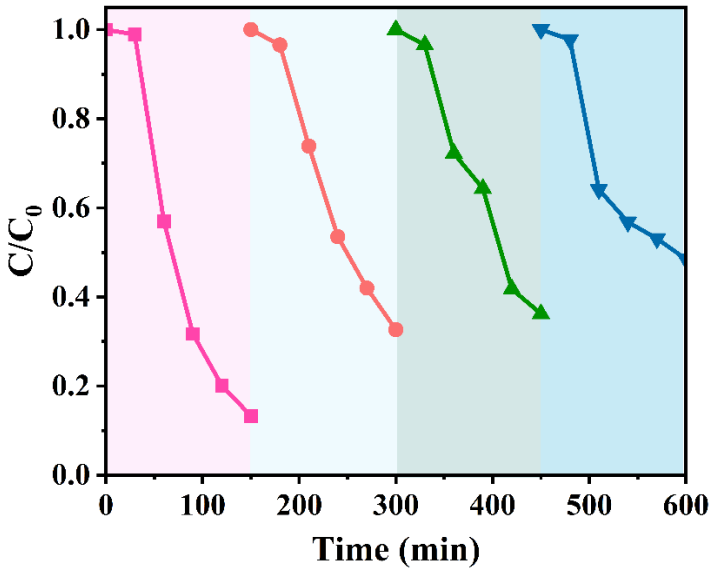

Fig. S18. C/C_0 cycle diagram of the BTO/PPy/TiO_2 under both ultrasonic and light.

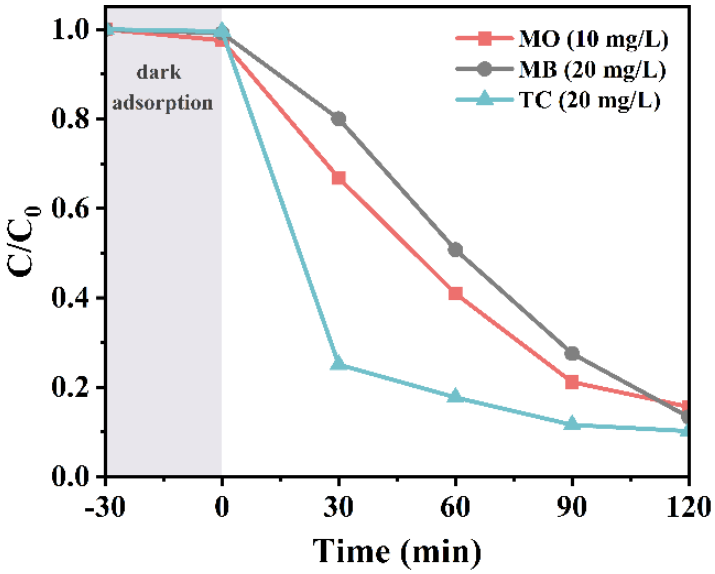

Fig. S19. The degradation performance of MO, MB, and TC for BTO/PPy/TiO_2 through photopiezocatalysis.

Table S1. Bader charge analysis of the PPy/BTO.

electron transfer number	C	N	H	O	Ti	Bi
|0.8501|	2.8365	-4.82	2.8336	-32.5066	16.998	14.658

Table S2. Bader charge analysis of the PPy/TiO_2.

electron transfer number	C	N	H	O	Ti
|0.88784|	2.8835	-4.80946	2.8138	-58.0156	57.128

Table S3. Literature comparison of photopiezocatalysts for RhB degradation.

Photopizeocatalysts	Catalyst dosage	Dye (RhB) / Concentration	Reaction conditions	Degradation rate	Ref.
$BiVO_4/BiFeO_3$	100 mg	5 ppm, 50 ml	Ultrasonic: 180 W, 40 kHz Light: Xenon lamp (λ>420 nm)	98% (120 min)	3
$KNbO_3/WO_3$	50 mg	10 ppm, 50 ml	Ultrasonic: 120 W, 40 kHz Light: Xenon lamp 210 W (780 nm>λ>400 nm)	98% (80 min)	4
PVDF/TiO_2/CQDs	26.6 mg	20 ppm, 25 mL	Longer Pump (24 mL min^{-1}) Light: Xenon lamp 300 W (λ>420 nm)	95.26% (100 min)	5
$BaTiO_3$@TiO_2	50 mg	30 ppm, 100 mL	Ultrasonic: 200 W, 45/ 80/100 kHz Light: Xenon lamp 300 W	99.5% (75 min)	6
$BaTiO_3$	50 mg	10 ppm, 50 mL	Ultrasonic: 300 W, 40 kHz Light: Xenon lamp 300 W	About 85% (60 min)	7
Se nanowires/Au	2 mg	2.5 × 10^{-3} mg/L, 10 ml	Ultrasonic: 100 W, 40 kHz Light: 1-sun (AM 1.5 G, 100 mW cm^{-2})	About 38% (30 min)	8

$NaNbO_3/WO_3$	25 mg	10 ppm, 100 mL	Ultrasonic: 180 W, 40 kHz Light: Xenon lamp 300 W (λ>420 nm)	73.7% (120 min)	[9]
This work BTO/PPy/TiO_2	**50 mg (including copper mesh, and the mass of the catalysts roughly equels 1 mg)**	**20 ppm, 20 mL**	**Ultrasonic: 240 W, 40 kHz** **Light: Xenon lamp 300 W (1000 W m^{-2})**	**96% (120 min)**	

References

1 C. Wang, F. Chen, C. Hu, T. Ma, Y. Zhang and H. Huang, *Chemical Engineering Journal*, 2022, **431**, 133930.

2 S. C. Chang, P.-H. Chen, Y.-C. Chen and J. M. Wu, *International Journal of Hydrogen Energy*, 2024, **50**, 15–25.

3 Q. Jing, Z. Liu, X. Cheng, C. Li, P. Ren, K. Guo, H. Yue, B. Xie, T. Li, Z. Wang and L. Shu, *Chemical Engineering Journal*, 2023, **464**, 142617.

4 R. Huang, W. Cai, H. Zhang, Z. Wang, Q. Zhang, R. Gao, G. Chen, X. Deng, X. Lei, J. Dong, X. Liu and C. Fu, *Journal of Environmental Chemical Engineering*, 2023, **11**, 110177.

5 Z. Tian, Y. Xu, Q. Liu, X. Wu, S. Qin, J. Zhang, H. Wang, J. Li and Z. Cui, *Surfaces and Interfaces*, 2024, **46**, 104056.

6 M. Kim, J. Kwon, H. J. Lee, K. S. Park, J. Kim, J. Kim, K. Baek, H. Yuan, J. K. Hyun, Y. S. Cho, J. Yeom and D. H. Kim, *Nano Energy*, 2022, **92**, 106702.

7 Q. Xiao, L. Chen, Y. Xu, W. Feng and X. Qiu, *Applied Surface Science*, 2023, **619**, 156794.

8 M. Kim, J. Kwon, H. J. Lee, K. S. Park, J. Kim, J. Kim, K. Baek, H. Yuan, J. K. Hyun, Y. S. Cho, J. Yeom and D. H. Kim, *Nano Energy*, 2023, **114**, 108680.

9 X. Yan, S. Zhang, L. Pan, T. Ai, Z. Li and Y. Niu, *Inorganic Chemistry Communications*, 2023, **158**, 111510.